

NIST Technical Note 1676

**Fabrication, Characterization, and
Flammability Testing of Multi-walled
Carbon Nanotube Layer-by-layer
Coated Polyurethane Foam**

Rick Davis
Yeon Seok Kim

NIST Technical Note 1676

**Fabrication, Characterization, and
Flammability Testing of Multi-walled
Carbon Nanotube Layer-by-layer
Coated Polyurethane Foam**

Rick Davis
Yeon Seok Kim
*Fire Research Division
Building and Fire Research Division*

September 2010



U.S. Department of Commerce
Gary Locke, Secretary

National Institute of Standards and Technology
Patrick D. Gallagher, Director

Certain commercial entities, equipment, or materials may be identified in this document in order to describe an experimental procedure or concept adequately. Such identification is not intended to imply recommendation or endorsement by the National Institute of Standards and Technology, nor is it intended to imply that the entities, materials, or equipment are necessarily the best available for the purpose.

National Institute of Standards and Technology Technical Note 1676
Natl. Inst. Stand. Technol. Tech. Note 1676, 31 pages (September 2010)
CODEN: NTNUE2

Abstract

The research presented here is the first report of fabricating multi-walled carbon nanotube (MWCNT) based thin coatings on polyurethane foam (PUF) using Layer-by-layer (LbL) assembly, and using MWCNTs to reduce the flammability of PUF. The (440 ± 47) nm thick four trilayer coatings of polyacrylic acid (anionic layer), polyethyleneimine functionalized MWCNTs (MWCNT-PEI, cationic layer), and polyethyleneimine (cationic layer) contained (50 ± 1) mass fraction % MWCNT. These thin film coatings completely and uniformly coated all the internal and external surfaces of the PUF. Other than very sparsely populated micron sized aggregates of MWCNT and nanometer sized surface cracks, the surfaces appeared smooth at low magnifications in the Scanning Electron Microscope (SEM). A sea of well dispersed and distributed MWCNTs completely embedded in the coating matrix was observed at high magnifications in the SEM. The thin MWCNT coatings significantly reduced the flammability of PUF; i.e., $55\% \pm 6\%$ reduction in peak heat release rate and $21\% \pm 3\%$ reduction in total burn time. This reduction from the coatings is comparable to what has been achieved with carbon nanofiber (CNF) coated PUF (using LbL) and is 50% better than reported for CNFs embedded directly into the PUF and 25% to 60% better than reported for other flame retarding technologies currently used in PUF. Critical to successfully fabricating high quality MWCNT coatings using LbL, retaining MWCNT during the coating process, and significantly reducing the flammability of PUF was first functionalizing the MWCNTs using one of the coating polymers, PEI.

Keywords

Layer-by-layer assembly; thin films; multi-walled carbon nanotubes; polyurethane foam; Cone Calorimetry; flammability; soft furnishings

Acknowledgements

Appreciation is extended to Dr. Alexander Morgan of the University of Dayton Research Institute for assisting with Cone Calorimetry and Prof. Jaime Grunlan from Texas A&M for his assistance with the Layer-by-layer coatings.

Contents

Abstract	iv
Acknowledgements	vi
List of Tables	ix
List of Figures	x
List of Acronyms	xii
1. Introduction	1
2. Experimental	2
2.1. Materials	2
2.1.1. Polyelectrolyte stock solutions of PEI (cationic) and PAA (anionic)	3
2.1.2. MWCNT-PEI cationic suspension	3
2.2. MWCNT coating methodology	3
2.3. CNF coating characterization	5
2.3.1. Scanning Electron Microscopy (SEM).....	6
2.3.2. Thermal Gravimetric Analysis (TGA)	6
2.3.3 Cone Calorimetry (Cone).....	6
3. Results and Discussion	6
3.1. MWCNT coating morphology.....	6
3.2. MWCNT/PUF thermal analysis and fire performance	10
3.2.1. Comparison to CNF/PUF	13
3.2.2. Comparison to other flame retarding technologies.....	13
4. Conclusion	14
5. Future Research	15
6. References	15

List of Tables

Table 1. Provided are the average physical characteristics of MWCNT/PUF. The (50 ± 1) mass fraction % MWCNT in the (440 ± 47) nm thick coating resulted in a (3.4 ± 0.4) mass fraction % increase in the PUF mass. Total MWCNT loading was (1.8 ± 0.1) mass fraction % of the MWCNT/PUF mass. These values are comparable to previously reported CNF coatings on PUF, except the CNF coatings were $28\% \pm 8\%$ thinner.[28] All values are reported with 2σ standard uncertainty.....	4
Table 2. Cone Calorimetry data of the PUF and MWCNT/PUF samples. The MWCNT coating resulted in a $55\% \pm 6\%$ reduction in Total Heat Release Rate (THR) and a $51\% \pm 5\%$ reduction in peak Heat Release Rate (PHRR). The MWCNT/PUF only had one PHRR, which was more of a plateau than a peak since the HRR was fairly consistent from $23 \text{ s} \pm 2\text{s}$ to $96 \text{ s} \pm 3 \text{ s}$. The PHRR and THR values of MWCNT/PUF are comparable to values previously measured for CNF/PUF.[28] All values are reported with 2σ standard uncertainty.....	13

List of Figures

- Figure 1. The MWCNT/polymer coating process was an alternating submersion in an anionic (PAA) solution, cationic (MWCNT-PEI) and another cationic (PEI only) solution with washing (rinse and wring) between each solution. After creating five trilayers (a PAA layer, MWCNT-PEI layers, and PEI layer), the specimen was dried in a convection oven for 12 h at $70\text{ }^{\circ}\text{C} \pm 1\text{ }^{\circ}\text{C}$ to remove excess water.....4
- Figure 2. Experimental layout for the coating process. The PAA (anionic) layer was deposited and excess PAA was removed by rinsing in containers 1a to 3a. The MWCNT-PEI (cationic) layer was then deposited and excess MWCNT-PEI was removed by rinsing in containers 1c to 3c. The last layer in the trilayer was PEI (cationic), which was deposited in the PEI container and the excess PEI was removed in rinsing containers 1C to 3C. This trilayer deposition process was repeated four more times in order to fabricate the five trilayer MWCNT coated PUF.....5
- Figure 3. SEM images of as-received PUF at (a) 1x, (b) 2x, (c) 5x, (d) 10x, (e) 20x, (f) 50x and (g) 100x and washed PUF at (h) 5x. The PUF surface contained a significant amount of debris (dust, etc.) that was removed upon washing (h). The wall surface was smooth and featureless. The edges of some struts are wavy due to recoiling of material from breaking the membrane during the PUF manufacturing.8
- Figure 4. SEM image of a washed PUF showing that the thin film of polymer forming the cell membrane can collapse onto the cell walls when the PUF sets during manufacturing. A membrane is still intact on the right side of the image.....9
- Figure 5. SEM images of the inside section of a MWCNT coated foam at (a) 1x, (b) 2x, (c) 5x, (d) 10x, (e) 20x (f) 50x, (g) 100x, (h) 200x, and (i) 500x. The box inserts represent the area in the next higher magnification image. The MWCNTs were well dispersed and distributed throughout the polymer coating. The coating was smooth and featureless except for a few small larger aggregates and a few $10\text{ nm} \pm 5\text{ nm}$ wide cracks. Values are reported with 2σ standard uncertainty.....10
- Figure 6. SEM images of the inside section of a MWCNT coated foam at (a) 50x, (b) 100x, (c) 200x, and (d) 500x. The MWCNT coating was $440\text{ nm} \pm 47\text{ nm}$ based on 12 measurements of seven different MWCNT/foam specimens. The cracks in the coating were significantly larger than those observed in the pre-fractured specimens, appeared rougher, and were primarily

located near the fracture surface; therefore, we assumed the fracture process created these cracks. The box inserts represent the area in the next higher magnification image. Values are reported with 2σ standard uncertainty.....11

Figure 7. Heat release rate (HRR) curves from Cone experiments of the washed standard PUF and the MWCNT/PUF. The MWCNT coating resulted in a $55\% \pm 6\%$ reduction in PHRR, $51\% \pm 5\%$ reduction in THR, and a $21\% \pm 3\%$ reduction in total burn time. The 2σ standard uncertainty is $\pm 5\%$ in HRR and ± 2 s in time.13

List of Acronyms

ANPR	Announced notice of proposed rulemaking
ASTM	American Society for Testing Materials
BF	Barrier fabric
BL	Bilayer
CNF	Carbon nanofibers
CNF/PUF	Carbon nanofiber coated standard polyurethane foam
CPSC	Consumer Product Safety Commission
DI	Deionized (water)
LbL	Layer-by-layer assembly/coating
MWCNT	Multi-walled carbon nanotubes
MWCNT/PUF	Multi-walled carbon nanotubes coated standard polyurethane foam
NIST	National Institute of Standards and Technology
PAA	Poly(acrylic acid)
PEI	Branched Polyethyleneimine
PHRR	Peak heat release rate
PUF	Standard polyurethane foam
SEM	Scanning Electron Microscopy
TGA	Thermogravimetric analysis
THR	Total heat released
TL	Trilayer

1. Introduction

The estimated annual societal cost of soft furnishing (mattresses and upholstered furniture) fires to the United States economy is \$5 billion [1,2,3,4]. These soft furnishings as the first item ignited fires account for 5% of all residential fires annually, but are responsible for a disproportionately high portion of the fire losses (33% of the civilian fatalities, 18% of civilian injuries, and 11% of the property losses). Over the next decade, federal flammability performance regulations are expected to significantly reduce these soft furnishing fire losses [5,6,7]. Soft furnishing manufacturers are and will likely continue to comply with these current and proposed flammability regulations by using fire blocking barrier fabrics. Despite this compliance, engineering and technical options to comply are quickly diminishing because of mandated sustainability regulations, such as REACH [8] and EcoLabel [9], for consumer products. Using Layer-by-layer assembly to create a fire resistant armor on the components in soft furnishings is being evaluated in this project as a novel technology to enable soft furnishings to comply with flammability and sustainability regulations.

Layer-by-layer (LbL) assembly has been extensively studied for the past 20 y as a methodology to create multifunctional films generally less than 1 μ m thick [10,11,12]. The thin film coatings were commonly fabricated through alternate deposition of a positively charged layer and negatively charge layer (called a bilayer, BL). By taking advantage of electrostatic [13], H-bonding [14], covalent bonds [15], and/or donor/acceptor interactions, these bilayers were continuously assembled on the surface of substrates. The LbL process is quite flexible and robust, which allows it to be tuned for specific coating characteristics and for coating a range of substrate types. For example, altering the concentration, pH, and/or temperature of the LbL solutions can result in a 1 nm rather than 100 nm thick BL [16,17].

LbL thin films have been used in an extensive breadth of applications, such as oxygen barriers [18] and sensors [19], and have useful properties, such as antimicrobial [20] and antireflection [21]. A more recent application, which is directly aligned with the research presented in this manuscript, was LbL clay coatings (sodium exchanged montmorillonite) on cotton fabric to improve the fire performance characteristics of this textile [12]. Clay has been extensively studied in LbL thin films [18,22,23] and, when used as an additive filler, has been shown to simultaneously improve the mechanical and fire performance attributes of polymers [24,25,26]. The uniqueness of Li's research is the concept of improving fire performance by using LbL assembly and creating assembled clay coatings on cotton fabric (clay/cotton) [12]. The results are exciting in that uniform high quality clay based coatings on cotton were achieved. In addition, the clay coatings resulted in a significant retention of fabric like char after conducting vertical burn tests and there was no (or less) ember afterglow when the flame was removed. These results suggest the coating may better prevent thermal and flame penetration from reaching and igniting the polyurethane foam (PUF), and therefore, the clay/cotton may reduce fire spread in residential homes if used in soft furnishings.

Two other recent publications closely connected with this research were using carbon nanofibers (CNFs) to reduce the flammability of polyurethane foam (PUF). Zammarano [27] measured a 35% reduction in peak heat release rate (PHHR) by incorporating 4 mass fraction % CNFs

directly into the PUF (CNFs included the foam recipe). In comparison, by coating the PUF with CNFs using LbL assembly, Davis [28] reported a 55% reduction in PHRR using only 1.7 mass fraction % CNFs. Although the CNF distribution was not completely uniform, the CNF network formed by the LbL deposition was sufficient to significantly reduce the peak heat release rate (PHRR), total heat release (THR), and total burn time, as compared to the pure PUF and the CNF-PUF nanocomposite. This pioneering work was the first time LbL assemblies made with CNFs were shown to improve the fire performance of PUF [28].

Compared to CNFs, carbon nanotubes (CNT) are significantly smaller in dimension. Single-walled carbon nanotubes (SWCNT) and multi-walled carbon nanotubes (MWCNT) have received a lot of attention in the science community because their inherent characteristics, such as small size and high aspect ratio (diameter of 1 nm to 100 nm and length of 1 μm to 100 μm for SWCNT and MWCNT, respectively) [29,30], high modulus (approximately 1 TPa) [31], high intrinsic electrical conductivity ($\sigma > 10^4$ S/cm) [32], and high thermal conductivity ($k > 1000$ W/m·K) [33], are expected to impart electrical conductivity, mechanical strength, and thermal conductivity to a polymer when the CNTs are incorporated into the polymer. However, CNTs continue to be underutilized partially due to the difficulties in generating stabilized CNT suspensions. To improve stability researchers have used noncovalent stabilizing agents (eg. surfactants [34,35,36], water-soluble polymers [37,38,39], and inorganic nanoparticles [40,41]) and chemically modified CNTs. For electrical conductivity, non-covalent stabilization of CNTs is preferred over covalent functionalizing because chemical modification has been shown to reduce conductivity [42,43,44]. On the other hand, covalent functionalizing shows better solubility due to the strong interfacial interaction between the nanotubes and polymer matrix via direct chemical bonding.

The research presented here is unique in that it is the first report of reducing PUF flammability using LBL assemblies fabricated with MWCNTs. Provided are the details of fabricating trilayer (TL) MWCNT coatings on polyurethane foam (MWCNT/PUF) using LbL, the physical characteristics of the LbL fabricated MWCNT coatings on PUF, the fire performance of PUF and MWCNT/PUF, and a comparison of MWCNT/PUF to CNF/PUF.

2. Experimental [45,46,47]

2.1. Materials

All materials were used as-received from the supplier unless otherwise indicated. Branched polyethylenimine (PEI, branched, $M_w = 25,000$ g/mol) and poly(acrylic acid) (PAA, $M_w = 100,000$ g/mol) were obtained from Sigma-Aldrich (Milwaukee, WI). These polymers were selected primarily because their behavior in LbL assembly is well documented and understood. Baytubes C150HP multi-walled carbon nanotubes (MWCNT, average diameter was 14 nm, length was 1 μm to 10 μm) were obtained from Bayer MaterialScience AG (Pittsburgh, Pennsylvania). The standard (untreated) polyurethane foam [48] coated in this study was stored as-received from the supplier (cardboard box with no packaging material at $25 \text{ }^\circ\text{C} \pm 2 \text{ }^\circ\text{C}$). On the day of coating, nine substrates (length/width/height of (10.2 cm / 10.2 cm / 5.1 cm) ± 0.1 cm) were cut from a single substrate (length/width/height of (30.6 cm / 30.6 cm / 5.1 cm) ± 0.1 cm). These smaller substrates were rinsed and wringed out (discussed below in the coating

process) to remove debris and other extractables (0.6 mass fraction % \pm 0.1 mass fraction %). After drying, the post-extraction mass of these substrates was 12.7 g \pm 0.3 g.

2.1.1. Polyelectrolyte stock solutions of PEI (cationic) and PAA (anionic)

The polyelectrolyte (0.10 mass fraction % \pm 0.03 mass fraction %) and deionized (DI, $< 0.5 \mu\text{S}$) water solutions were prepared as follows. A 2 L glass container was charged with DI water (1300 mL) and PEI (0.10 mass fraction % \pm 0.03 mass fraction %, 1.3 g \pm 0.4 g). This PEI cationic stock solution was slowly agitated for 6 h at room temperature before using. The preparation of the PAA anionic stock solution was similar to the PEI cationic solution, except PAA (0.10 mass fraction % \pm 0.03 mass fraction %, 1.3 g \pm 0.4 g) was used instead of PEI. The pH value was 10 and 3 for the PEI and PAA solutions, respectively.

2.1.2. MWCNT-PEI cationic suspension

The MWCNTs were first functionalized with PEI to facilitate dispersion and distribution in DI water and to improve retention of the MWCNTs in the coating. Amination of MWCNTs was prepared according to the procedure by Liao et al [49]. A plastic vial (500 mL) was charged with *N,N*-dimethylformamide (200 mL \pm 1 mL, DMF), PEI (5.0 mass fraction % \pm 0.1 mass fraction relative to DMF, 10 g \pm 0.1 g), and MWCNT (20.0 mass fraction % \pm 0.1 mass fraction % relative to PEI, 2.0 g \pm 0.1 g). The mixture was sonicated at 40 watts for 1 h then agitated with a stir bar for at least 2 d at 50 °C \pm 2 °C. The functionalized MWCNT product (MWCNT-PEI) was isolated from the suspension by filtering through a 0.20 μm nylon membrane and washing four times with alternating methanol and water washes to remove excess PEI and DMF. The MWCNT-PEIs were dried in a dessicator with anhydrous calcium sulfate for at least 3 d prior to use. The dried product was a powder that appeared to be slightly larger than the as-received MWCNTs.

The MWCNT-PEI in DI water suspension was prepared by charging a plastic bottle (250 mL) with DI water (150 mL \pm 1 mL) and MWCNT-PEI (0.10 mass fraction % \pm 0.03 mass fraction % relative to total DI water, 0.60 g \pm 0.02 g). The suspension was sonicated at 40 watts for 1 h with the temperature never exceeding 70 °C \pm 1 °C then was diluted with more DI water (450 mL) and shaken by hand for 3 min \pm 1 min. The MWCNT-PEI suspension was used immediately for coating the PUF.

2.2. MWCNT coating methodology

MWCNT/PUF fabrication took approximately 40 min per specimen (20 min for the first TL and 20 min for the remaining four TL). In general, the fabrication process was alternately depositing an anionic layer (PAA), a functionalized MWCNT only cationic layer (MWCNT-PEI), and a polymer only cationic layer (PEI) on the surface of the PUF and removing unbound material (MWCNT and polymer) by rinsing with DI water and wringing out the excess water several times (Figure 1). The process of removing excess water using a convection oven and dessicator occurred over a period of 3 d.

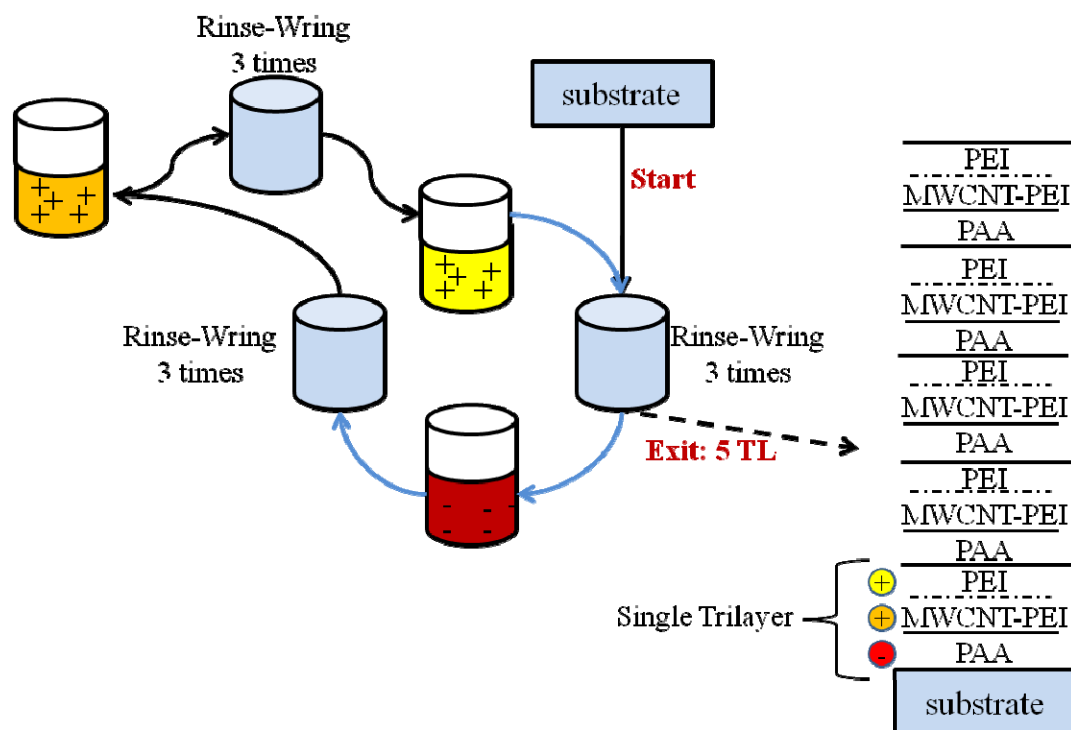


Figure 1. The MWCNT/polymer coating process was an alternating submersion in an anionic (PAA), MWCNT cationic (MWCNT-PEI) and polymer cationic (PEI only) solutions with washing (rinse and wring) between each solution. After creating five TL (a PAA layer, MWCNT-PEI layer, and PEI layer), the specimen was dried in a convection oven for 12 h at $70\text{ }^{\circ}\text{C} \pm 1\text{ }^{\circ}\text{C}$ to remove excess water.

More specifically, three plastic containers (2 L) were charged with the coating solutions. One container (2 L) was charged with the PAA anionic solution ($600\text{ mL} \pm 10\text{ mL}$), a second with the MWCNT-PEI cationic suspension ($600\text{ mL} \pm 10\text{ mL}$), and a third with the PEI cationic solution ($600\text{ mL} \pm 10\text{ mL}$) (Figure 2). Three rinsing containers (2 L) per coating solution were charged with DI water ($600\text{ mL} \pm 10\text{ mL}$, each). A PUF substrate was submersed into the PAA anionic solution and after squeezing and releasing the substrate four times, the substrate was soaked in the PAA solution for an additional 5 min. The substrate was removed and the excess solution was squeezed back into the anionic dipping container.

To remove unbound PAA, the substrate was thoroughly rinsed in three separate containers (Figure 2). Since most of the PAA was typically removed in the first rinsing container (Figure 2 #1a), the rinsing water in this container was replaced with fresh deionized water after each washing cycle. Excess water was removed by passing the substrate twice through Dyna-Jet BL-44 hand wringer (Dyna-Jet Products, Overland Park, KS).

The MWCNT-PEI cationic layer was then deposited onto the PAA/PUF specimen and the unbound MWCNT-PEI was removed using the same procedure described above, except the washings were performed using #1c, #2c, and #3c rinsing containers. The polymer only cationic layer (PEI only) was then deposited onto the MWCNT-PEI/PAA/PUF specimen and washed

using the same procedures described above, except using the #1C, #2C, and #3C rinsing containers. This deposition of a PAA layer, a MWCNT-PEI layer, and a PEI layered created a single TL (PEI/MWCNT-PEI/PAA/PUF). The procedure for depositing the next four TLs was the same as the first TL, except the substrate was only soaked in the coating solutions for 1 min rather than 5 min. After the coating was complete, the specimen was dried in a convection oven ($70\text{ }^{\circ}\text{C} \pm 1\text{ }^{\circ}\text{C}$, 12 h) and then stored in a dessicator (at least 3 d) with anhydrous calcium sulfate before weighing and analyzing. The purpose of using functionalized MWCNTs and a trilayer coating will be explained in the Results and Discussion section.

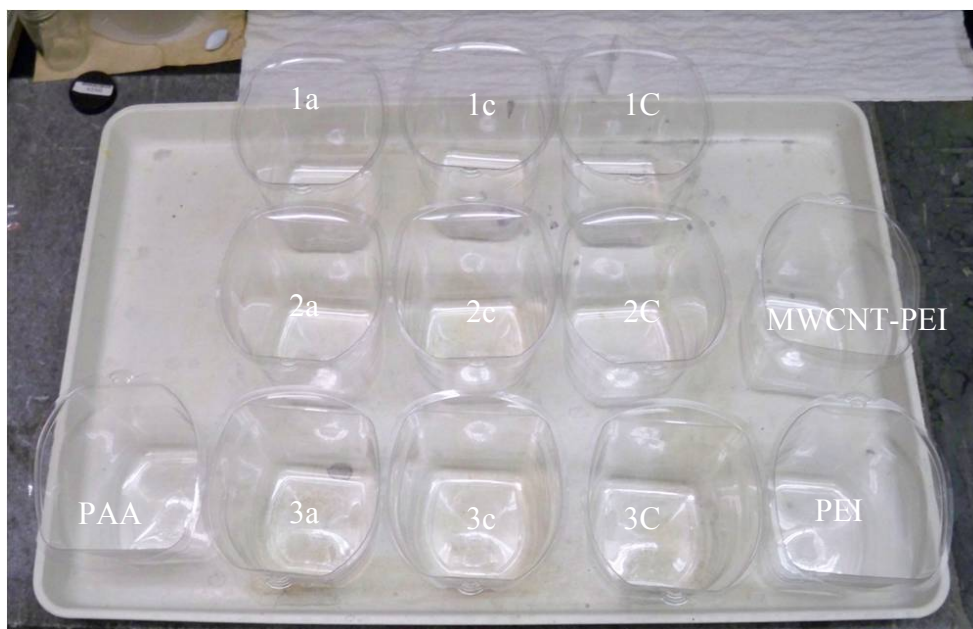


Figure 2. Experimental layout for the coating process. The PAA (anionic) layer was deposited and excess PAA was removed by rinsing in containers 1a to 3a. The MWCNT-PEI (cationic) layer was then deposited and excess MWCNT-PEI was removed by rinsing in containers 1c to 3c. The last layer in the trilayer was PEI (cationic), which was deposited in the PEI container and the excess PEI was removed in rinsing containers 1C to 3C. This trilayer deposition process was repeated four more times in order to fabricate the five trilayer MWCNT coated PUF.

2.3. CNF coating characterization

All measured values are reported with a 2σ uncertainty, unless otherwise indicated. The physical characteristics of the MWCNT/PUF are provided in Table 1. The increase in substrate mass due to the coating (Mass fraction % coating) was measured using a laboratory microbalance. The amount of MWCNTs in the coating (Mass fraction % CNF in coating) was calculated from

Table 1. Provided are the average physical characteristics of MWCNT/PUF. All values are reported with 2σ standard uncertainty.

Mass (g)	Mass fraction % coating	Mass fraction % CNF on CNF/PUF	Mass fraction % CNF in coating	Coating thickness (nm)
13.2 ± 0.3	3.4 ± 0.4	1.8 ± 0.1	50 ± 1	440 ± 47

2.3.1. Scanning Electron Microscopy (SEM)

A Zeiss Ultra 60 Field Emission-Scanning Electron Microscope (FE-SEM, Carl Zeiss Inc., Thornwood, NY) was used to collect images of the CNF coatings, from which, the coating thickness was approximated (Table 1), and the distribution of nanoparticles and overall quality of the LbL coating was inspected. All SEM samples were sputter coated with 4 nm of Au/Pd (60 mass fraction %/40 mass fraction %) prior to SEM imaging.

2.3.2. Thermal Gravimetric Analysis (TGA)

A Q-500 GA Thermal Gravimetric Analyzer (TGA, TA Instruments, New Castle, DE) was used to measure the concentration of CNF on the substrates (Table 1, Mass fraction % CNF on CNF/PUF). The samples ($20 \text{ mg} \pm 3 \text{ mg}$) were placed on a ceramic pan ($250 \mu\text{L}$, TA Instruments) then loaded into the furnace by the autosampler. Under a nitrogen atmosphere, the temperature was stabilized at $90 \text{ }^\circ\text{C} \pm 1 \text{ }^\circ\text{C}$ (30 min) then ramped to $800 \text{ }^\circ\text{C} \pm 2 \text{ }^\circ\text{C}$ at $10 \text{ }^\circ\text{C}/\text{min}$. The reported CNF content was based on the remaining mass fraction % at $600 \text{ }^\circ\text{C}$. All values are reported with 2σ standard uncertainty.

2.3.3 Cone Calorimetry (Cone)

A dual Cone Calorimeter (Cone, Fire Testing Technology, East Grinstead, United Kingdom), operating at $35 \text{ kW}/\text{m}^2$ with an exhaust flow of $24 \text{ L}/\text{s}$, was used to measure the fire performance of uncoated and CNF coated PUF. The experiments were conducted according to standard testing procedures (ASTM E-1354-07). A $((10.2 \text{ cm} / 10.2 \text{ cm} / 5.1 \text{ cm}) \pm 0.1 \text{ cm})$ sample was placed in a pan constructed from aluminum foil. The pan was slightly larger than the test sample and the pan sides were flared away from the sample. This allowed the sides as well as the top of the sample to be exposed during testing. Following the methodology developed by Zammarano [50], the Cone data was normalized to account for a change in surface area of the specimens during testing. When exposed to the external heat flux, the PUF melted and the MWCNT/PUF shrank slightly. By the end of the experiment, the MWCNT/PUF had an two times larger average surface area than the PUF melt pool. Therefore, the MWCNT/PUF data presented here was reduced by a factor of 2. All values are reported with 2σ standard uncertainty ($\pm 5\%$ in HRR and $\pm 2 \text{ s}$ in time).

3. Results and Discussion

3.1. MWCNT coating morphology

In order to fabricate MWCNT coatings that contained a high concentration of well distributed MWCNTs, the MWCNTs needed to form a stable suspension in the depositing solution and adhere to the surface of the coated PUF. Initially, a stable MWCNT suspension was attempted using PEI or sodium deoxycholate surfactant. After sonicating for three hours, the MWCNTs appeared well dispersed and stable, but the suspension rapidly destabilized over one hour. Qualitatively, the coatings fabricated of PUF from these solutions had low content and non-uniform distribution of MWCNTs (non-uniform and mostly light gray color after six bilayers). A drastic improvement resulted from using MWCNTs functionalized with PEI [49].

The MWCNT-PEI formed a stable suspension in DI over several days without the need for a stabilizing surfactant. The coatings fabricated on PUF with the MWCNT-PEI were a uniform black color after six bilayers suggesting a higher content and more uniform distribution of MWCNTs compared to using PEI or sodium deoxycholate. However, during the coating process the MWCNT-PEI would transfer from the PUF into the PAA depositing solution (PAA solution became gray). This suggested poor adhesion of the MWCNT-PEI to PAA likely due to the MWCNT-PEI having a relatively weak charge. Rather than working to improve adhesion, the problem of MWCNT-PEI retention was addressed by depositing a PEI layer after the MWCNT-PEI (creating a TL) as the adhesion was then based more on pure PAA and PEI interactions, which strongly adhere to each other.

SEM was used to characterize the LbL fabricated MWCNT coatings on PUF. Other than dust and debris on the surface of the PUF, the as-received PUF surface appears smooth and featureless even at high magnification (Figure 3). Prior to depositing the first layer, the PUF was washed with DI water, which completely removes all of the debris (Figure 3h). The wavy edges of the PUF walls are a result of the manufacturing process. The PUF was initially closed cell with a very thin polyurethane membrane connecting the walls. When the membrane was “popped” to form this open cell structure, there was a slight relaxation of the strained edges of the walls and the membrane snapped back onto the walls which created the wavy appearance observed in Figure 3h.

The images of the MWCNT/PUF in Figure 4 are of a section near the center of a MWCNT/PUF specimen and representative of the type of coatings observed on specimens. At low SEM magnifications, the surface appears to be void of MWCNTs other than a few sparsely populated MWCNT aggregates that are on the order of tens of micron in size (Figure 4a through Figure 4e). Higher magnifications (Figure 4e through Figure 4h) reveals the PUF surface was completely covered with a uniform coating, which contained well distributed MWCNTs completely embedded in the polymer coating. A few small surface cracks ($10 \text{ nm} \pm 5 \text{ nm}$) are observed and are believed to result from the drying process. These types of cracks are common in thicker LbL coatings. It was assumed that these surface cracks would not deteriorate the fire performance of the MWCNT/PUF; therefore, there was no further investigation of the cracks.

SEM images of a fractured MWCNT/PUF were taken with the fracture surface in the plane of the image, which provides cross sectional views of the PUF and the coating (Figure 5). The MWCNT coating was $440 \text{ nm} \pm 47 \text{ nm}$ thick based on seven measurements taken on each of 12 different MWCNT/PUF specimens. The surface morphology at low magnifications is consistent with that observed in Figure 4 (high MWCNT uniformly distributed and completely embedded in polymer). The cracks in this MWCNT coating are assumed to have resulted from the fracturing process, because they are an order of magnitude larger than any cracks observed prior to fracturing, are primarily located at the fracture surface, and contain exposed MWCNTs.

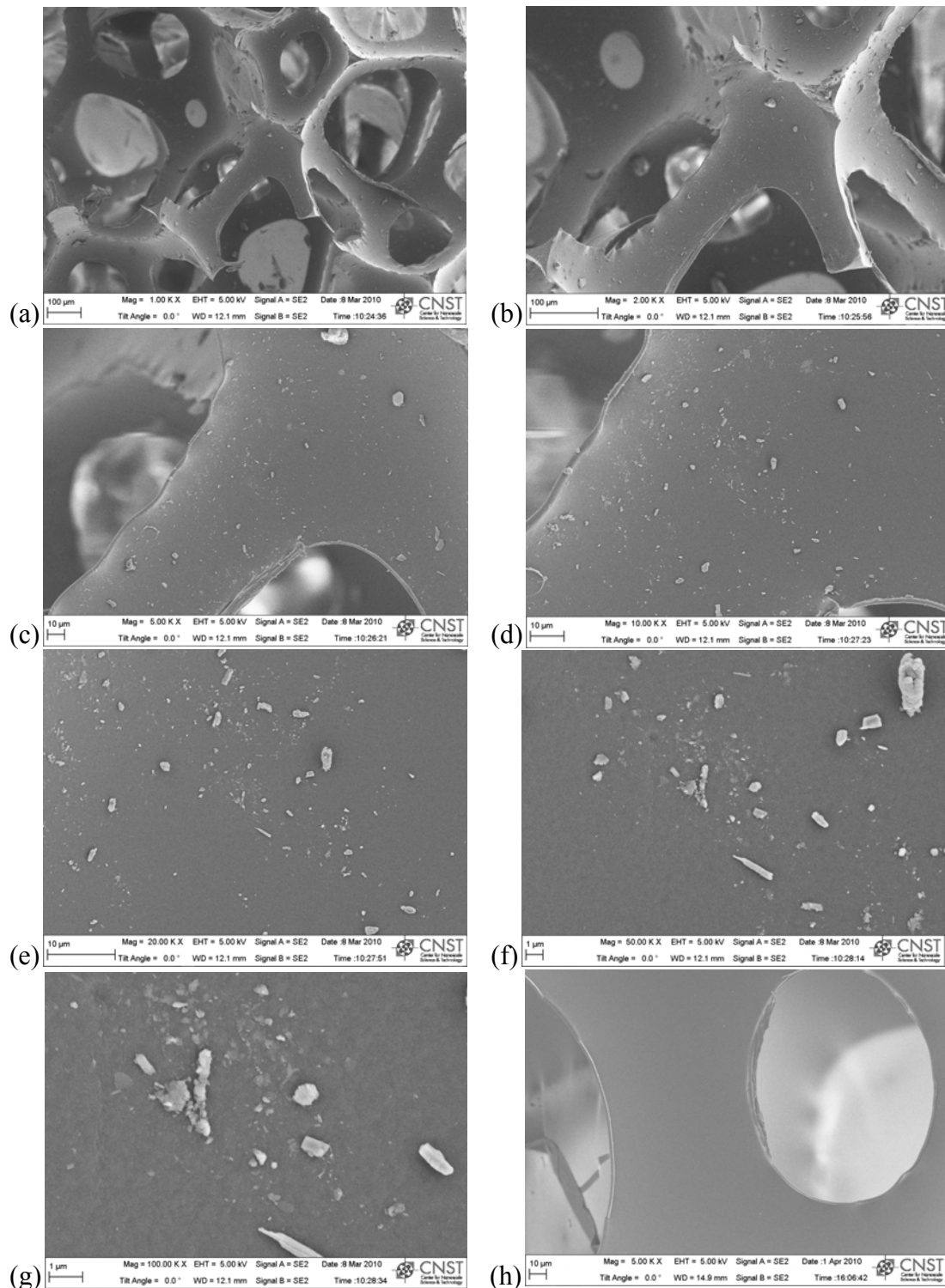


Figure 3. SEM images of as-received PUF at (a) 1x, (b) 2x, (c) 5x, (d) 10x, (e) 20x, (f) 50x and (g) 100x and washed PUF at (h) 5x. The PUF surface contained a significant amount of debris (dust, etc.) that was removed upon washing (h). The wall surface was smooth and featureless. The edges of some struts are wavy due to recoiling of material from breaking the membrane and/or shrinkage from solvent loss during the PUF manufacturing.

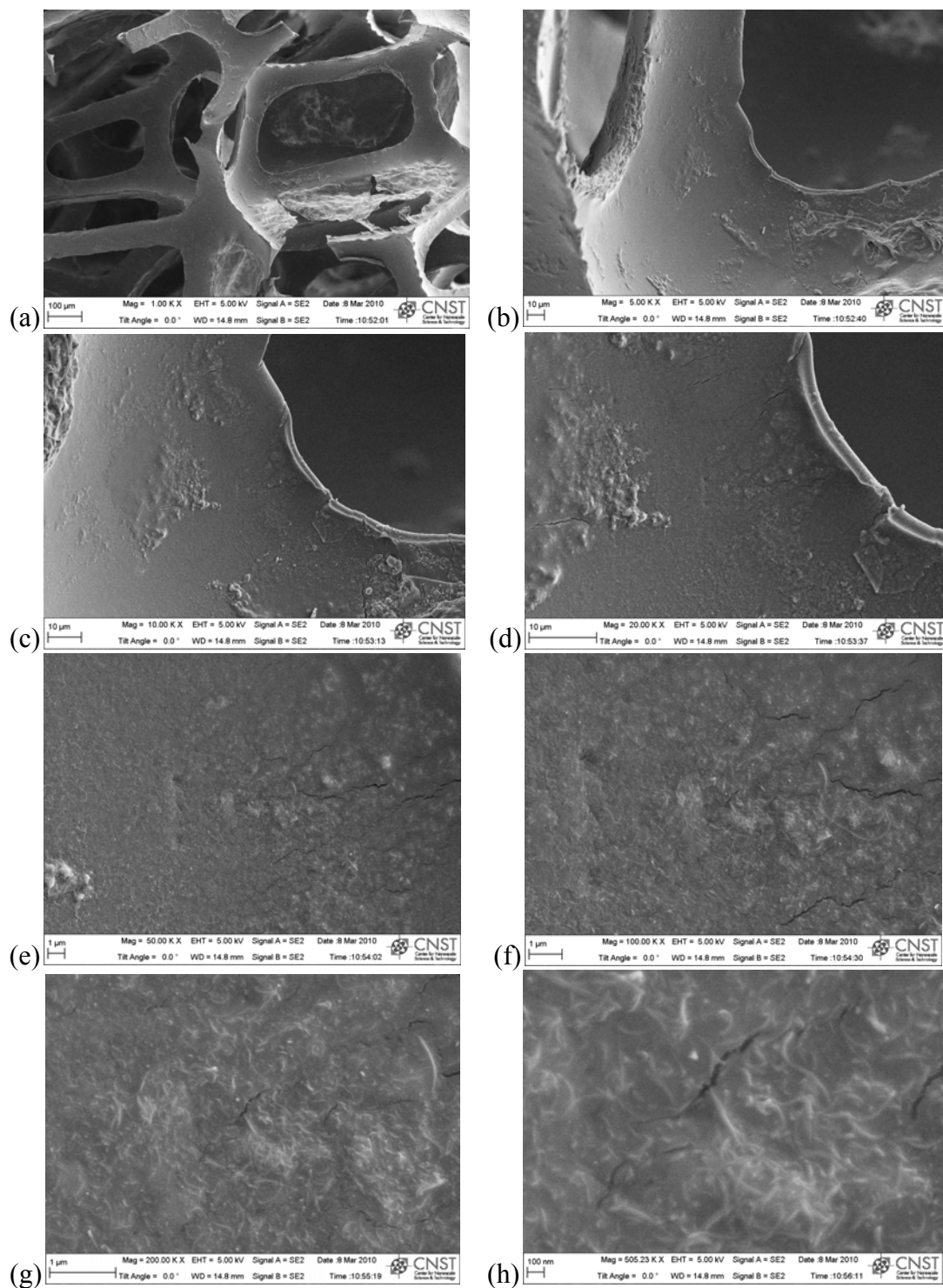


Figure 4. SEM images of the inside section of a MWCNT coated foam at (a) 1x, (b) 5x, (c) 10x, (d) 20x, (e) 50x (f) 100x, (g) 200x, and (h) 500x. The MWCNTs were well dispersed and distributed throughout the polymer coating. The coating was smooth and featureless except for a few small larger aggregates and a few $10 \text{ nm} \pm 5 \text{ nm}$ wide cracks. Values are reported with 2σ standard uncertainty.

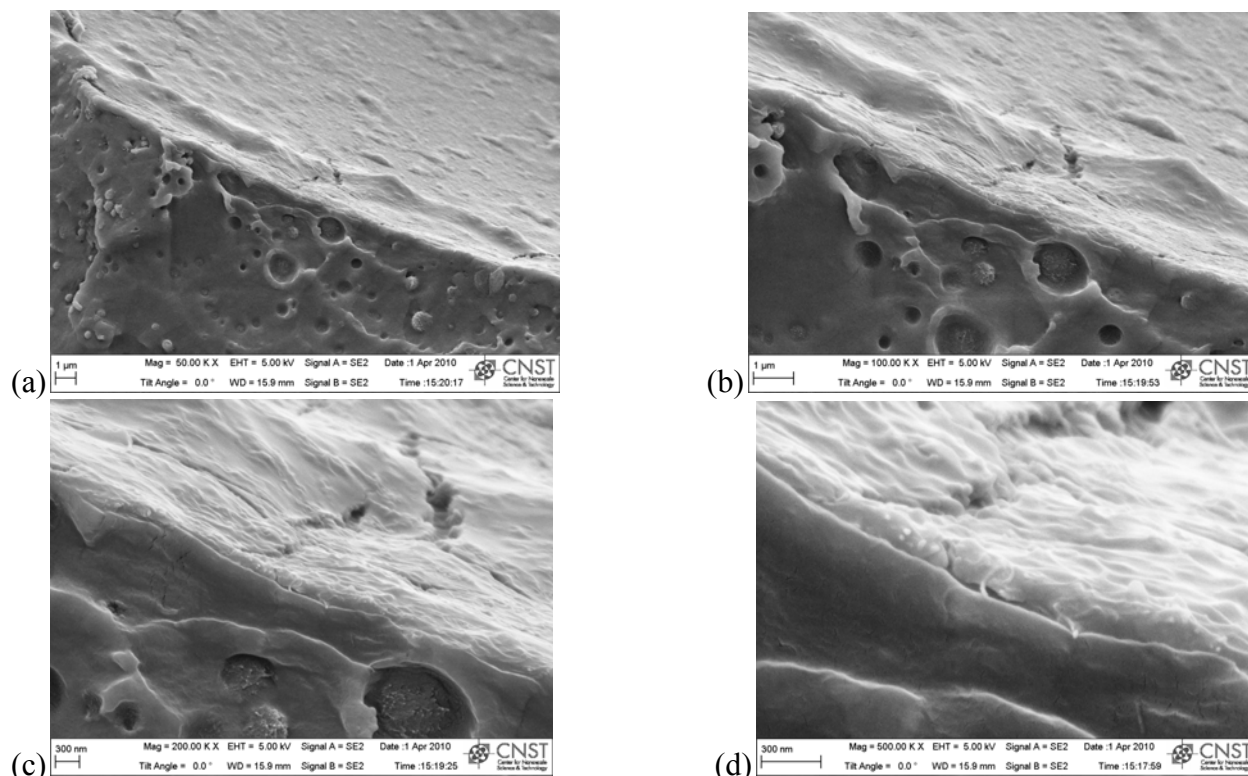


Figure 5. SEM images of the inside section of a MWCNT coated foam at (a) 50x, (b) 100x, (c) 200x, and (d) 500x. The MWCNT coating was $440 \text{ nm} \pm 47 \text{ nm}$ based on seven measurements of 12 different MWCNT/foam specimens. The cracks in the coating were significantly larger than those observed in the pre-fractured specimens, appeared rougher, and were primarily located near the fracture surface; therefore, we assumed the fracture process created these cracks. Values are reported with 2σ standard uncertainty.

3.2. MWCNT/PUF thermal analysis and fire performance

TGA and a microbalance were used to determine the actual mass of MWCNTs and coating deposited onto the substrates. The five TL MWCNT coatings increase the mass of the substrate by $3.4 \text{ mass fraction } \% \pm 0.4 \text{ mass fraction } \%$, of which, $51 \text{ mass fraction } \% \pm 1 \text{ mass fraction } \%$ is MWCNTs. The total MWCNT content relative to the substrate mass is $1.8 \text{ mass fraction } \% \pm 0.1 \text{ mass fraction } \%$, which is a typical loading level of carbon nanotubes or nanofibers incorporated into polymers (not a coating) to improve the polymer's fire performance. Unlike these other nanocomposites, the MWCNTs in these coatings are concentrated at the surface rather than randomly dispersed and distributed throughout the polymer matrix [28].

Cone is a routine bench scale fire test that simulates a developing fire scenario on a small specimen and is used to measure the forced burning fire performance of polymers. The parameters reported from the test, such as time to ignition of the combustion gases (TTI), the time to peak and the peak maximum heat release rate (PHRR), and the total heat release (THR), are directly related to the potential fire threat of the burning polymer. The values of these parameters are the bases of the performance metrics for several existing or proposed national fire regulations. Cone heat release rate measurements are referenced to sample surface area (kW/m^2). The raw data collected in this study was adjusted as the surface area of the PUF and

MWCNT/PUF changed during the test. More specifically, the uncoated PUF melts to form a pool fire (flaming drips began at $27 \text{ s} \pm 2 \text{ s}$, all PUF was a pool fire at $40 \text{ s} \pm 2 \text{ s}$) with an exposed surface dimensions of $10.2 \text{ cm} \pm 0.1 \text{ cm}$ by $10.2 \text{ cm} \pm 0.1 \text{ cm}$. In contrast, the MWCNT/PUF only shrank (no melting) during the test because of the MWCNT network created by the LbL coating. The average surface area of the MWCNT/PUF at the end of the experiments is two times larger than the average PUF pool fire surface area. In other words, the same fuel load was spread over twice the surface area in the MWCNT/PUF. All exposed surfaces (top and sides) of the MWCNT/PUF were contributes to the HRR while only the top surface of the PUF pool fire contributes to HRR. The surface area adjusted Cone heat release curves indicate the five TL MWCNT coatings significantly reduce the flammability of PUF (Figure 6 and Table 2). The $440 \text{ nm} \pm 47 \text{ nm}$ MWCNT-based coating that resulted in $50.3 \text{ mass fraction } \% \pm 0.1 \text{ mass fraction } \% \text{ MWCNT loading on PUF causes a decrease of}$

- $55\% \pm 6\%$ in the PHRR ($435 \text{ kW/m}^2 \pm 26 \text{ kW/m}^2$ to $197 \text{ kW/m}^2 \pm 11 \text{ kW/m}^2$),
- $51\% \pm 5\%$ in the THR ($33 \text{ MJ/m}^2 \pm 2 \text{ MJ/m}^2$ to $16 \text{ MJ/m}^2 \pm 1 \text{ MJ/m}^2$), and
- and $22\% \pm 2\%$ in total burn time ($158 \text{ s} \pm 2 \text{ s}$ to $\text{LbL } \text{s} \pm 2 \text{ s}$),

as compared to PUF.

Unlike the PUF, the MWCNT/PUF has a steady state HRR from $27 \text{ s} \pm 2 \text{ s}$ to $95 \text{ s} \pm 2 \text{ s}$ ($185 \text{ kW/m}^2 \pm 15 \text{ kW/m}^2$). This suggests the coating yields a more controlled/steady combustion of the polyurethane. A significant reduction in PHRR value and/or loss of a PHRR is common behavior in char forming materials. The char forms a protective layer (armor) surrounding the substrate, which thermally protects the substrate and reduces/prevents the volatile combustion products from contributing as fuel to the fire. The post-Cone residual mass (char yield) is five times higher for the MWCNT/PUF specimens ($11.1 \text{ mass fraction } \% \pm 0.4 \text{ mass fraction } \% \text{ as compared to } 2.2 \text{ mass fraction } \% \pm 0.1 \text{ mass fraction } \% \text{ for the MWCNT/PUF and PUF, respectively}$). Adjusting for MWCNT content and PUF char yield, and assuming a negligible impact of the PEI and PAA polymers, the MWCNT/PUF resulted in $8.1 \text{ mass fraction } \% \pm 0.4 \text{ mass fraction } \% \text{ increase in non-pyrolized polymer (e.g. char yield)}$. The improved fire performance of MWCNT/PUF measured in the Cone is partially attributed to this increased char yield; however, the primary driver is the shape retention and hence the two times larger burning surface area of the MWCNT/PUF.

As indicated previously, the PUF melts to form a pool fire, whereas, the MWCNT/PUF retains most of its original dimensions. In a real fire scenario and full scale tests, the formation of a pool fire approximately increases the fire threat (as calculated from HRR, THR, and burn time) of the burning product by 35% [51]. This impact is not captured in Cone data because there is no product (soft furnishing, etc.) for the pool fire to pose an additional flux upon. With this in mind, the Cone data is a conservative measure of the improved fire performance created by the MWCNT coating, but the actual benefit in real fires from using a MWCNT/PUF instead of PUF, could be 35% greater than that reported here.

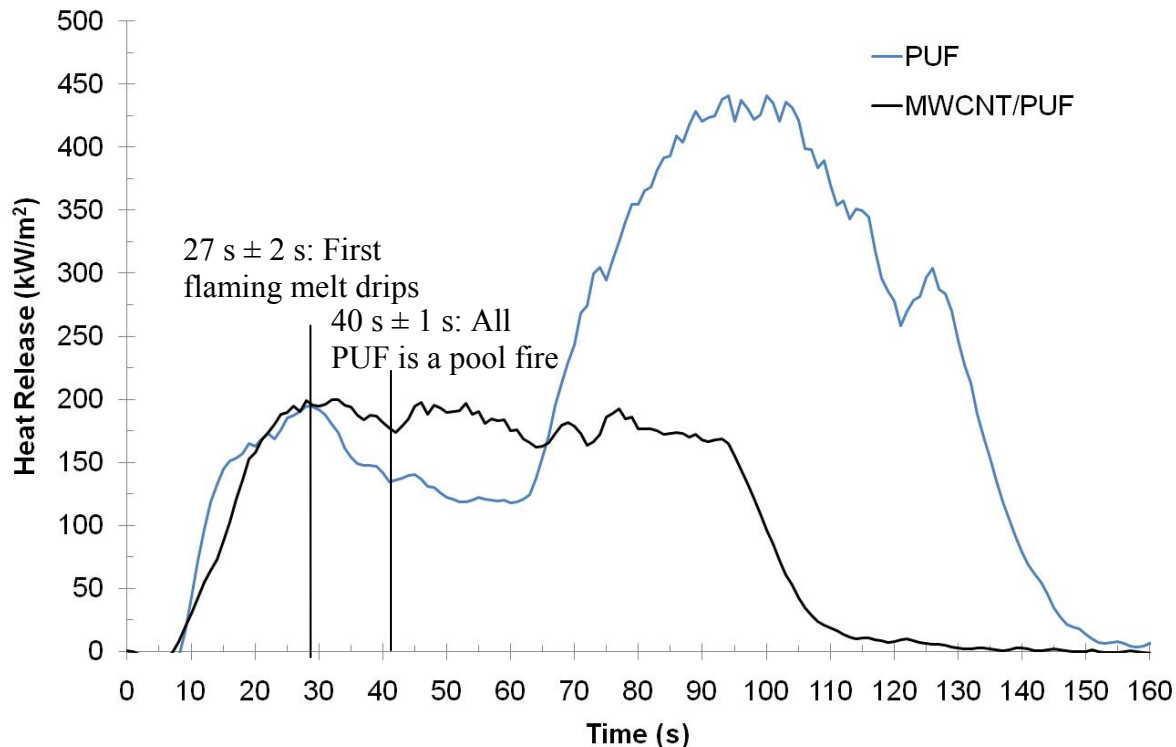


Figure 6. Heat release rate (HRR) curves of the washed standard PUF and the MWCNT/PUF. The five TL MWCNT coating resulted in a $55\% \pm 6\%$ reduction in PHRR, $51\% \pm 5\%$ reduction in THR, and a $21\% \pm 3\%$ reduction in total burn time. The 2σ standard uncertainty is $\pm 5\%$ in HRR and ± 2 s in time.

Table 2. Cone Calorimetry data of the PUF and MWCNT/PUF samples. The approximate $52\% \pm 6\%$ reduction in PHRR and THR on PUF resulting from the MWCNT coatings is comparable to the values measured for CNF coatings on PUF ($55\% \pm 6\%$) [28]. All values are reported with 2σ standard uncertainty.

	Peak 1		Peak 2		THR	Residue Mass	Burn time
	HRR (kW/m²)	Time (s)	HRR (kW/m²)	Time (s)	(MJ/m²)	Fraction %	(s)
PUF	194 ± 10	28 ± 2	435 ± 22	103 ± 3	33 ± 2	2.2 ± 0.1	158 ± 2
MWCNT/PUF	197 ± 4	28 ± 2	---	---	16 ± 1	11.1 ± 0.4	123 ± 2

3.2.1. Comparison to CNF/PUF

The characteristics of the previously reported CNF-based coatings on PUF are distinctly different to what is reported here for MWCNT. More specifically, the MWCNT coatings completely and uniformly cover the entire surface of the PUF and, other than a few sparsely distributed tens of micron sized MWCNT aggregates, the coating appears smooth and featureless at lower magnifications. In contrast, the CNF-based coatings are rougher with an appearance more similar to a fibrous network rather than a smooth, uniform coating [28]. The coatings cover all the PUF surfaces. Due to its large dimensions the fibers tend to deposit as groups rather than individual fibers, which results in regions of high (tens of microns in size) and regions of no (less than a few microns in size) CNFs. The highly aggregated regions contain fibers that are only partially embedded in the polymer coating. The regions of smaller aggregates (islands) generally contain fibers almost completely embedded in the polymer coating. The CNF and MWCNT loading in the coatings were the same (50 mass fraction % \pm 1 mass fraction %), but the CNF coating was 28% \pm 8% thinner than the MWCNT coating (359 nm \pm 36 nm as compared to 440 nm \pm 47 nm, respectively).

One of the major factors impacting the physical characteristics of the coatings is the stability of the coating preparation suspensions. It was reported that within 4 h of stopping sonication, the CNFs began to settle to the bottom of the depositing solution as indicated by a color gradient (darker at the bottom) in the CNF suspension [28]. During deposition the CNF suspension appeared very uniform. However, it was proposed that the reason the CNFs deposited as aggregates was because the CNFs had already begun to aggregate in the suspension. In comparison, the MWCNT suspensions in this study remained visibly uniform over two days. This difference in quality of the suspensions is most likely a result of the smaller dimensions and/or the PEI functionalizing of the MWCNT.

Even though the physical characteristics of the coatings were quite different, the improvement in PUF fire performance due to the CNF or MWCNT LbL fabricated coatings were very similar. More specifically, both coatings resulted in a 53% \pm 6% reduction in PHRR and THR, and 21% \pm 3% in total burn time. The primary reason for this drastic decrease in flammability is that the coatings prevent foam melt dripping and increase char formation.

3.2.2. Comparison to other flame retarding technologies

Najafi-Mohajeri used Cone to measure the impact of 17 flame retardant additive packages (five non-halogen, four halogen, and seven halogen-phosphorous) on the flammability of a standard PUF [52]. These additive packages are commercially available and reported to be commonly used by the PUF industry. The five non-halogens reduced the PUF PHRR and THR by an average of 15% and 14%, respectively. The best performing non-halogen additive was a silicone additive with amine functionality (Dow Corning® I-9641), which reduced PHR and THR by 40% and 6%, respectively, at a 3.3 mass fraction % loading. The four halogens reduced the PUF PHRR and THR by an average of 31% and 16%, respectively. The best performing halogen additive package was a pentabromodiphenyl oxide additive blend (Great Lakes DE-60F), which reduced PHRR and THR by 37% and 31%, respectively, at a 20 mass fraction % loading. The

seven halogen-phosphorous systems reduced the PUF PHRR and THR by an average of 14% and 7%, respectively. The best performing halogen-phosphorous additive package was a 28 mass fraction % halogenated phosphate ester (Great Lakes Firemaster® HP-36, 44.5% halogen and 5.5% phosphorous) and 7 mass fraction % antimony oxide (Laurel Industries), which reduced PHRR and THR by 43% and 7%, respectively.

Also using a Cone, Price [53] measured the flammability impact of incorporating melamine-based flame retardants into PUF. The exact composition materials are unknown as they were purchased from a supplier. The melamine and melamine chlorate phosphate blend reduced the PHRR by 10% and 15%, respectively. As an alternative to using flame retardants, the authors also measured the impact of using fire blocking barrier fabrics to reduce the PUF flammability. Of the six specimens tested, the best performing combination was wrapping the standard PUF with zirconium hexafluoride flame retardant treated wool (FR-wool), which gave a 29% reduction in PHRR. This FR-wool also gave the greatest reduction in PHRR of the flame retardant foams (32%), which was quite similar to what was reported for wrapping the standard PUF with this FR-wool. These results suggest the fire performance benefits gained by using these flame retardants are partially mitigated by the FR-wool.

Compared to these competitor flame retardant (FR) systems, the MWCNT coatings developed in this project delivers a greater reduction in PHRR and/or THR (12% to 44%) using a significantly lower amount of FR (1.6 mass fraction % CNF, as compared to 3 mass fraction % to 35 mass fraction % of these commercial FRs [52,53]). This reduction in PHRR and THR for the MWCNT/PUF was 18% and 20% greater, respectively, than measured for the best performing halogen flame retardant filled PUF and 12% and 44% greater, respectively, than measured for the best performing halogen-phosphorous flame retardant filled PUF. Compared to melamine chlorate phosphate filled PUF and FR-wool wrapped PUF, the reduction in PHRR for the CNF/PUF was 40% and 22% greater, respectively.

4. Conclusion

For the first time, LbL assemblies made with MWCNTs are shown to improve the fire performance of polyurethane foam. The process described here generates 440 nm \pm 47 nm thick PAA/MWCNT-PEI/ PEI trilayer-based coatings containing 51 mass fraction % \pm 1 mass fraction % MWCNT that are well and uniformly distributed across all of the internal and external surfaces of the porous polyurethane foam. Other than isolated/sparsely populated MWCNT aggregates and small surface cracks, the MWCNT/PUF coatings are smooth and featureless. Critical to this LbL process is using PEI functionalized MWCNTs and depositing a layer of PEI between the MWCNT-PEI and PAA layers. This LbL coating significantly reduces the heat release rate, total heat release, and total burn time of the PUF with just five bilayers (e.g., 55% \pm 6% reduction in PHRR). Compared to FR systems commercially used to reduce PUF flammability and using CNF embedded in the PUF, these MWCNT-based coatings yield a significantly greater reduction in PUF flammability at a significantly lower additive concentration (e.g., 1.6 mass fraction % MWCNT coating on PUF yields a 20% lower THR than a 20 mass fraction % brominated FR in PUF). The reduction in PUF flammability by using LbL assembled CNFs-based coatings is the same as reported here for these MWCNT coatings. The MWCNT coatings also prevents the formation of a melt pool of burning foam, which in a real

fire scenario, may further reduce the resulting fire threat of burning soft furnishings in residential homes. This research lays the foundation for using LbL to fabricate coatings on foam and barrier fabrics using a range of nanoparticles and other performance-enhancing additives. Single-walled carbon nanotubes, clay, cellulosic fibers, and mixed additive coatings are currently being investigated on both foam and barrier fabrics. Additionally, the release of nanoparticles during aging and the change in fire performance due to aging are currently being measured.

5. Future Research

This research has laid the foundation for using LbL to fabricate coatings on foam and barrier fabrics using a range of nanoparticles and other performance enhancing additives. We are currently fabricating and analyzing clay coatings, cellulosic fiber coatings, and mixed additive coatings on both foam and barrier fabrics. In addition, we are measuring the release of nanoparticles during aging and measuring the change in fire performance due to aging.

6. References

-
- [1] J.R. Hall. Total cost of fire in the United States. National Fire Protection Association; February (2008). Summary available from:
<http://www.nfpa.org/assets/files/PDF/totalcostsum.pdf>.
 - [2] J.R. Hall, B. Harwood. The national estimates approach to U.S. fire statistics. *Fire Tech.* 25(2) (1989) 99-113.
 - [3] M. Greene, D. Miller. 2006-2008 Residential Fire Loss Estimates. Consumer Product Safety Commission report. August (2010). Available from: <http://www.cpsc.gov/library/fire06.pdf>.
 - [4] M. Ahrens. Home fires that began with upholstered furniture. National Fire Protection Association. May (2008). Summary available from:
<http://www.nfpa.org/assets/files/PDF/UpholsteredExecutiveSum.pdf>.
 - [5] 16 CFR 1632 Standard for the flammability of mattresses and mattress pads. Consumer Product Safety Commission. May (1991). Available from:
<http://www.cpsc.gov/businfo/testmatt.pdf>.
 - [6] 16 CFR 1633 Standard for the flammability (open flame) of mattress sets. Consumer Product Safety Commission. March (2007). Available from:
<http://www.cpsc.gov/businfo/frnotices/fr06/mattsets.pdf>.
 - [7] 16 CFR Part 1634, Standard for the flammability of residential upholstered furniture (proposed rule). Consumer Product Safety Commission. March (2008). Available from:
<http://www.cpsc.gov/businfo/frnotices/fr08/furnflamm.pdf>.
 - [8] http://echa.europa.eu/reach_en.asp
 - [9] <http://ec.europa.eu/environment/ecolabel/>
 - [10] Decher G. Chapter 1 Polyelectrolyte multilayers: An overview. *Multilayer Thin Films: Sequential Assembly of Nanocomposite materials*: G Dechner and JB Schlenoff (Eds.); Wiley-VCH: Weinheim, Germany, 2003.

-
- [11] Podsiadlo P, Shim BS, Kotov, NA. Polymer/clay and polymer/carbon nanotube hybrid organic-inorganic multilayered composites made by sequential layering of nanometer scale films. *Coordination Chemical Reviews*. 2009;253:2835-2851.
- [12] Li YC, Schulz J, Mannen S, Delhom C, Condon R, Chang S, Zammarano M, Grunlan JC. Flame retardant behavior of polyelectrolyte-clay thin film assemblies on cotton fabric. *ACS Nano*. 2010;4(6):33258-3337.
- [13] Y. Shimazaki, R. Nakamura, S. Ito, M. Yamamoto. Molecular Weight Dependence of Alternate Adsorption through Charge-Transfer Interaction. *Langmuir*. 17 (2001) 953-956.
- [14] Lv F, Peng ZH, Zhang LL, Yao LS, Xuan L. Photoalignment of liquid crystals in a hydrogen bonding directed Layer-by-layer ultrathin films. *Liquid Crystals*. 2009;36:43-51.
- [15] Bergbreiter DE, Chance BS. "Click"-Based covalent Layer-by-layer assembly on polyethylene using water soluble polymeric reagents. *Macromolecules*. 2007;40:5337-5343.
- [16] Mermut O, Barrett CJ. Effects of charge density and counterions on the assembly of polyelectrolyte multilayers. *Journal of Physical Chemistry B*. 2003;107:2525-2530.
- [17] Chang L, Kong X, Wang F, Wang L, Shen J. Layer-by-layer assembly of poly(N-acryloyl-N'-propylpiperazine) and poly(acrylic acid): effect of pH and temperature. *Thin Solid Films*. 2008;516:2125-2129.
- [18] Priolo MA, Gamboa D, Grunlan JC. Transparent clay-polymer nano brick wall assemblies with tailorable oxygen barrier. *ACS Applied Materials Interfaces*. 2010;2:312-320.
- [19] Aoki P, Volpati D, Riul A, Caetano W, Constantino CJL. Layer-by-layer technique as a new approach to produce nanostructured films containing phospholipids as transducers in sensing applications. *Langmuir*. 2009;25:2331-2338.
- [20] Fu JH, Ji J, Fan DZ, Shen JC. Construction of Antibacterial multilayer films containing nanosilver via Layer-by-layer assembly of heparin and chitosan-silver ions complex. *Journal Biomedical Material Research A*. 2008;79A:665-674.
- [21] Hiller J, Mendelsohn JD, Rubner MF. Reversibly erasable nanoporous antireflection coatings from polyelectrolyte multilayers. *Nature Materials*. 2002;1:59-63.
- [22] Podsiadlo P, Michel M, Lee J, Verploegen E, Kam NWS, Ball V, Lee J, Qi Y, Hart AJ, Hammond PT, Kotov NA. Exponential growth of LbL films with incorporated inorganic sheets. *Nano Letters*. 2008;8:1762-1770.
- [23] Li YC, Grunlan JC. Polyelectrolyte/nanosilicate thin-film assemblies: Influence of pH on growth, mechanical behavior, and flammability. *ACS Applied Materials Interfaces*. 2009;1:2338-2347.
- [24] Davis RD, Gilman JW, Vanderhart DL. Processing degradation of polyamide 6/montmorillonite clay nanocomposites and clay organic modifier. *Polymer Degradation and Stability*. 2003;79:111-121.
- [25] Gilman JW, Bourbigot S, Shields JR, Nyden M, Kashiwagi T, Davis RD, Vanderhart DL, Demory W, Wilkie CA, Morgan AB, Harris J, Lyon RE. High throughput methods for polymer nanocomposites research: extrusion, NMR characterization, and flammability property screening. *Journal of Materials Science*. 2003;38:4451-4460.

-
- [26] Davis RD, Lyon RE, Takemori MT, Eidelman N. Chapter 16 High throughput techniques for fire resistant materials development, *Fire Retardancy of Polymeric Materials 2nd Edition*. CA Wilkie and AB Morgan (Eds.): Taylor and Francis, Boca Raton, FL. 2010; p 421-451.
- [27] Zammarano M, Kramer RH, Harris RH, Ohlemiller TJ, Shields JR, Rahatekar SS, Lacerda S, Gilman JW. Flammability reduction of flexible polyurethane foams via carbon network formation. *Polymers for Advanced Materials*. 2008;19:588-595.
- [28] Davis RD, Kim YK. Impact of Carbon Nanofiber Layer-by-layer Coatings on Polyurethane Foam Flammability, National Institute of Standards and Technology Technical Note XXXX, in press. September 2010.
- [29] Nikolaev P. Gas-phase catalytic growth of single-walled carbon nanotubes from carbon monoxide. *Chemical Physics Letters*, 1999;313(1-2):91-97.
- [30] Coleman JN. Small but strong: A review of the mechanical properties of carbon nanotube-polymer composites. *Carbon*, 2006;44(9):1624-1652.
- [31] Yu M.F. Tensile loading of ropes of single wall carbon nanotubes and their mechanical properties. *Physical Review Letters*. 2000;84(24):5552-5555.
- [32] Thess A. Crystalline ropes of metallic carbon nanotubes. *Science*. 1996;273(5274):483-487.
- [33] Yu C. Thermal conductance and thermopower of an individual single-wall carbon nanotube. *Nano Letters*. 2005;5(9):1842-1846.
- [34] Fantini C. Investigation of the light emission efficiency of single-wall carbon nanotubes wrapped with different surfactants. *Chemical Physics Letters*. 2009;473(1-3):96-101.
- [35] Grossiord N. Toolbox for dispersing carbon nanotubes into polymers to get conductive nanocomposites. *Chemistry of Materials*. 2006;18(5):1089-1099.
- [36] Moore VC. Individually suspended single-walled carbon nanotubes in various surfactants. *Nano Letters*. 2003;3(10):1379-1382.
- [37] Yu C. Thermoelectric Behavior of Segregated-Network Polymer Nanocomposites. *Nano Letters*. 2008;8(12):4428-4432.
- [38] Kang YK. Helical Wrapping of Single-Walled Carbon Nanotubes by Water Soluble Poly(p-phenyleneethynylene). *Nano Letters*. 2009;9(4):1414-1418.
- [39] Zou JH. Dispersion of pristine carbon nanotubes using conjugated block copolymers. *Advanced Materials*. 2008;20(11):2055-2071.
- [40] Liu L, Grunlan JC., Clay assisted dispersion of carbon nanotubes in conductive epoxy nanocomposites. *Advanced Functional Materials*. 2007;17(14):2343-2348.
- [41] Zhu J. Dispersing carbon nanotubes in water: A noncovalent and nonorganic way. *Journal of Physical Chemistry B*. 2004;108(31):11317-11320.
- [42] Liu L. Comparison of Covalently and Noncovalently Functionalized Carbon Nanotubes in Epoxy. *Macromol Rapid Communications*. 2009;30(8):627-632.
- [43] Lafuente E. The influence of single-walled carbon nanotube functionalization on the electronic properties of their polyaniline composites. *Carbon*. 2008;46(14):1909-1917.
- [44] Bartholome C., Influence of surface functionalization on the thermal and electrical properties of nanotube-PVA composites. *Composites Science and Technology*. 2008;68(12):2568-2573.

-
- [45] Certain commercial equipment, instruments or materials are identified in this paper in order to specify the experimental procedure adequately. Such identification is not intended to imply recommendation or endorsement by the National Institute of Standards and Technology, nor is it intended to imply that the materials or equipment identified are necessarily the best available for this purpose.
- [46] The policy of NIST is to use metric units of measurement in all its publications, and to provide statements of uncertainty for all original measurements. In this document however, data from organizations outside NIST are shown, which may include measurements in non-metric units or measurements without uncertainty statements.
- [47] In this document, we have provided link(s) to website(s) that may have information of interest to our users. NIST does not necessarily endorse the views expressed or the facts presented on these sites. Further, NIST does not endorse any commercial products that may be advertised or available on these sites.
- [48] Future Foam Inc, 2451 Cypress Way, Fullerton CA 92831-5103, 714-871-5103.
- [49] Liao K, Wan A, Batteas JD, Bergbreiter DE. Superhydrophobic Surfaces Formed Using Layer-by-layer Self-Assembly with Aminated Multi-walled Carbon Nanotubes. *Langmuir*. 2008 Apr 1;24(8):4245-4253.
- [50] M. Zammarano. BFRL Foam Flammability Consortia homepage, <http://www.bfrl.nist.gov/866/foam/>. [cited 2010 July 20].
- [51] Pitts WM, Haspias G, Macatangga P, Fire spread and growth on flexible polyurethane foam. Eastern States Section of the Combustion Institute Fall 2009. University of Maryland, College Park, MD. October 18-21, 2009; p. 11-22.
- [52] N. Najafi-Mohajeri, C. Jayakody, G.L. Nelson. Cone Calorimetric Analysis of Modified Polyurethane Elastomers and Foams with Flame-Retardant Additives. *Fire and Polymers*. American Chemical Society; 2010; p 79-89. Available from: <http://dx.doi.org/10.1021/bk-2001-0797.ch007>
- [53] D. Price, Y. Liu, R. Hull, G.J. Milnes, B.A. Kandola, A.R. Horrocks. Burning behavior of fabric/polyurethane foam combinations in the cone calorimeter. *Polym. Intern.* 49 (2000) 1153-1157.